SUPPLEMENTARY METHODS

BrdU and EdU labeling

For *in vivo* pulse/chase BrdU labeling experiments, recently hatched first-instar larvae were collected and grown in standard medium at 25°C. At the desired developmental time, larvae were collected again and transferred to multiwell plates and fed for 2.5 h with fruit juice containing 1 mg/ml BrdU and a red alimentary dye. Subsequently, larvae that incorporated substantial red dye in the guts were returned to standard medium to complete their development until white pupae or 24 h after adult eclosion. Larval brains were dissected in Ringer's solution and fixed for 3 min with modified Carnoy's fixative followed by 75% EtOH for 30 min. After rehydration, the samples were denatured by treatment with 2 N HCl for 40 min and then extensively washed with PBS before proceeding to IHC analysis with anti-BrdU antiserum (Beckton-Dickinson), followed with a HRP-conjugated secondary antiserum and finally revealed with DAB. To detect BrdU incorporation in adult brains, anesthetized flies were decapitated, and the heads were rapidly embedded in Tissue-Tek (Miles, Elkhart, IN) and frozen instantaneously with liquid nitrogen. Frontal 12 µm sections were obtained with a microtome cryostat and they were immediately fixed with cold 4% paraformaldehyde. After denaturation with 2 N HCl for 30 min, tissue sections were washed with PBS and processed for immunostaining with anti-BrdU as above.

In vitro BrdU labeling of larval brains was performed essentially as described previously (Tejedor et al., 1995; Ceron et al., 2001) but with incubation times of 5-10 min. At this end, larval brains were quickly dissected in freshly prepared Ringer solution along no more than 12 min. Eye-antenna discs were keep attached to the brains to avoid alterations in OL morphology. Brain samples were then transferred to a small well containing the BrdU (35 µ/ml). or EdU (20µM; stock: 20mM in DMSO) in Riger's.

For BrdU detection, samples were processed as described above. For a cellular analysis, labelled larval brains were post-fixed with osmium tetroxide and embedded in SPURR, as described previously (Rogero et al., 1997). Subsequently, ultramicrotome sections (3 µm) were counterstained with 0.25% toluidine blue in 0.5% borax for 2-5 min at 60 °C, and contrasted with 75% EtOH for 5 min. These short BrdU pulses label reproducibly and strongly the OPC and CB NBs but not the IPC was not consistently labelled.

For EdU detection**,** after a very quick wash with Ringer solution, samples were fixed with ice cold 4% paraformaldehyde/0.1% Triton-X100 during 60min and permeabilized with PBS/0.5% Triton X-100 for 30 min at RT. Finally, they were washed with PBS/0.1% Triton X-100 just before proceeding to the Click-iT reaction (Life Technologies) under standard conditions.

Production and purification of anti-Mnb antiserum

We raised an antiserum (called MNB-NTH) against the N-terminal region of all MNB protein isoforms following a procedure similar to that described by Tejedor et al. (1995). In brief, we produced a fusion protein by subcloning a *mnb* cDNA fragment (between Sal I and HindIII sites containing the N-terminal region of all Mnb protein isoforms) into the pGEXT-2T plasmid. The fusion protein was expressed in bacteria under standard conditions and purified by preparative SDS-PAGE electrophoresis and electroelution. The purified protein was used to immunize rabbits using standard methods. The resulting crude antiserum was affinity purified using a fusion protein prepared with the same cDNA fragment inserted into the pUR 288 expression vector. The specificity of this affinity-purified antiserum was confirmed by WB and IHC using larval brains of LoF and GoF *mnb* alleles.

Immunohistochemistry

Larval brains were dissected in ice cold PBS along no more than 15 min. and fixed for 30 min on ice with 4% paraformaldehyde in PBS, and then for a further 30 min with 4% paraformaldehyde, 0.1% Triton X-100 in PBS. For antisera that had serious problems penetrating the tissue, larval brains were embedded in 4% low-melting-point agarose, and 50 µm sections were obtained with a vibratome. Brains or sections were saturated with incubated with primary antisera overnight at 4–8°C plus 1h at RT in PBS containing 5% normal goat serum, 0.1% Triton X-100 and 0.02% sodium azide. After extensive washing with 5 mg/ml BSA in PBS/0.1% Triton X-100, samples were incubated with Fluorescent (Alexa-488; Alexa-594, Alexa-647, Cy2, Cy3 or Cy5)-, biotin-, or HRP- coupled secondary antibodies (Jackson Immunochemicals) at 1:400-800 dilutions in 5 mg/ml BSA in PBS/0.1% Triton X-100 for 2h at RT. Cy2- or Cy3-conjugated streptavidin was used for the detection of biotinylated secondary antibodies, while labeling of HRP-conjugated secondary antibodies was revealed with Cy2, Cy3 or Cy5 TSA (Perkin Elmer). Immunolabelled samples were analyzed on Leica TCS-SL or Olympus Fluoview FV1200 confocal microscopes.

Antibodies details.

All antibodies used in this report have been validated in previous studies.

Protein / antigen	Type	Host	Source	Reference.	Dilution
Ase	P	Rb	gift from YN Jan	Brand et al, 1993	1:2000
BrdU	M	Mo	Becton-Dickinson	Clone 3D4	1:100
Caspase3	P	Rt	Cell Signaling Tech.	Asp175	1:100
Cyc E	P	Rt	gift from H. Richardson	Crack et al., 2002	1:150
Dpn	P	Gp	gift from J. Skeath	Colonques et al, 2011	1:1500
Dpn	P	Rb	gift from YN Jan	Bier et al.,1992	1:500
Dpn	M	Rt	gift from C. Doe	Boone and Doe, 2008	1:50
DE-Cadherin	M	Rt	DSHB	Clone DCAD2	1/25
Elav	M	Rt	DSHB	Clone 7E8A10	1:200

GFP	P	Rb	Invitrogen	A11122	1:200
Grh	P	Rb	gift from H. Reichert	Bello et al., 2006	1:80
Mira	M	Mo	gift from F. Matsuzaki	Clon PLF81	1:20
Mira	P	Rb	gift from C. Gonzalez	Molinari et al., 2002	1:600
PatJ	P	Rb	gift from H. Bellen	Bhat et al., 1999	1:500
PH3	P	Rb	Upstate Biotechnology	06-570	1:500
Pros	M	Mo	DSHB	clone MR1A	1:40

Abbreviations: Gp=guinea pig, M=monoclonal, Mo=mouse, P=Polyclonal, Rb=rabbit, Rt=rat

Analysis of cell death

In addition to TUNEL, cell death was also monitored *in vivo* in the larval brain by Acridine orange staining in freshly dissected larval brains under experimental conditions previously used in larval imaginal discs (Abrams et al., 1993). Apoptosis was also detected with anti-activated Caspase 3 antibodies (Cell Signaling Technologies). The presence of pyknotic cells was analyzed by EM. At this end, larval brains were fixed with 4% paraformaldehyde/0.5% glutaraldehyde in PBS, post-fixed with 0.2% osmium tetroxide in PBS, and embedded in SPURR. Subsequently, 2 µm plastic sections were obtained with an ultramicrotome and stained with toluidine blue as described previously (Rogero et al., 1997). 80–90 nm ultramicrotome sections were obtained, contrasted with uranyl acetate and lead citrate, and finally, examined using an electron microscope (JEOL USA, Inc., Peabody, MA).

Quantitative image analysis.

For quantitative image analysis, mutant and control specimens were processed in parallel for IHC in the same experiment. Furthermore, samples were analyzed within the same work session using exactly the same acquisition parameters in the confocal microscope.

For quantitative determination of the density of labeled cells, partial projections of confocal serial sections were performed for equivalent regions (X,Y,Z axis) and counting of labeled cells was made by eye.

Quantitative determination of immune labeling intensity was carried out using the Image J program on unmodified images covering equivalent spatial regions (X,Y,Z axis) of mutant and control specimens.

Abbreviations

BrdU, bromodeoxyuridine; CB, central brain; DAB, diaminobenzidine ; DS, Down syndrome; EdU, 5-ethynyl-2′-deoxyuridine; FISH, fluorescent in-situ hybridization; GC, ganglion cell; GMC, ganglion mother cell; GoF, gain of function; LoF, loss of function; IHC, immunohistochemistry; NB, neuroblast; NP, neural progenitor ; OL, optic lobe; OPC, outer proliferation center; PBS, phosphate buffer saline; PFA, paraformaldehyde; PH3, phospho-histone-3; RT, room temperature

Supplementary References

Abrams JM, White K, Fessler LI, Steller H. 1993. Programmed cell death during Drosophila embryogenesis. Development. 117(1):29-43.

Almeida MS, Bray SJ (2005) Regulation of post-embryonic neuroblasts by Drosophila Grainyhead. Mech Dev 122(12): 1282–93

Bello B, Reichert H, Hirth F (2006) The brain tumor gene negatively regulates neural progenitor cell proliferation in the larval central brain of Drosophila. Development 133(14): 2639–2648.

Bier, E., Vaessin, H., Younger-Shepherd, S., Jan, L.Y., Jan, Y.N. (1992). deadpan, an essential pan-neural gene in Drosophila, encodes a helix-loop-helix protein similar to the hairy gene product. Genes Dev. 6(): 2137--2151.

Boone JQ, Doe CQ (2008) Identification of Drosophila type II neuroblast lineages containing transit amplifying ganglion mother cells. Dev Neurobiol 68(9): 1185–95.

Brand M, Jarman AP, Jan LY, Jan YN. (1993) asense is a Drosophila neural precursor gene and is capable of initiating sense organ formation. Development. 119(1):1-17.

Colonques J, Ceron J, Tejedor FJ (2007) Segregation of postembryonic neuronal and glial lineages inferred from a mosaic analysis of the Drosophila larval brain. Mech Dev 124(5): 327–40.

Colonques, J., Ceron, J., Reichert, H. and Tejedor, F. J. (2011). A transient expression of Prospero promotes cell cycle exit of Drosophila postembryonic neurons through the regulation of Dacapo. PLoS One 6, e19342.

Crack D, Secombe J, Coombe M, Brumby A, Saint R, Richardson H. (2002) Analysis of Drosophila cyclin EI and II function during development: identification of an inhibitory zone within the morphogenetic furrow of the eye imaginal disc that blocks the function of cyclin EI but not cyclin EII. Dev Biol. Jan 1;241(1):157-71.

Mollinari C, Lange B, González C. (2002) Miranda, a protein involved in neuroblast asymmetric division, is associated with embryonic centrosomes of Drosophila melanogaster. Biol Cell. 94(1):1-13.

O. Rogero, B. Hammerle and F.J. Tejedor (1997) Diverse expression and distribution of Shaker potassium channels during the development of the Drosophila nervous system. J. Neurosci.17, 5108-18

Tejedor F, Zhu XR, Kaltenbach E, Ackermann A, Baumann A, Canal I, Heisenberg M, Fischbach KF, Pongs O. (1995) minibrain: a new protein kinase family involved in postembryonic neurogenesis in Drosophila. Neuron. 14(2):287-301.

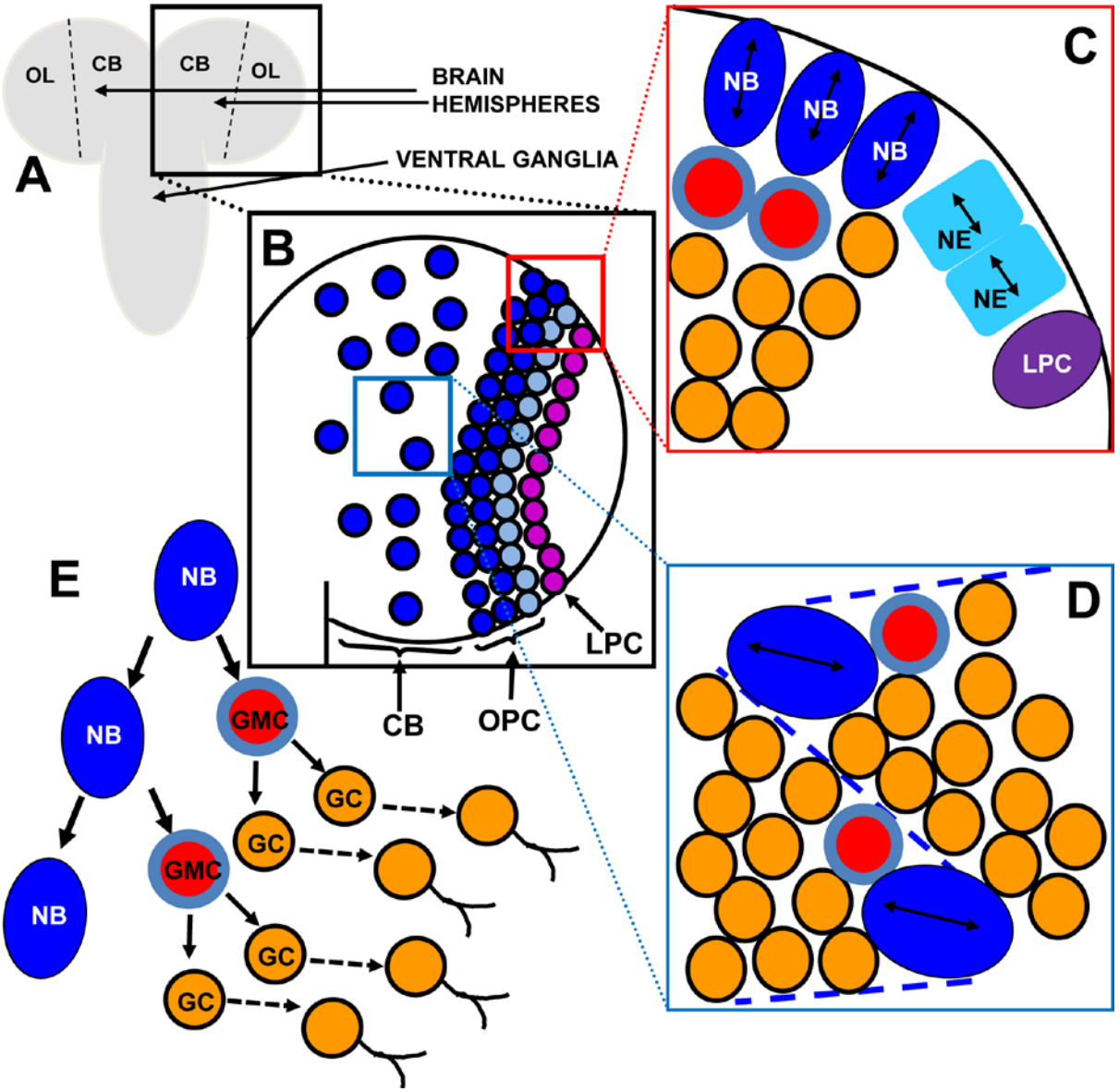

Suppl. Fig. S1. Morphology, cellular organization and pattern of division in the larval brain hemispheres.

A. Schematic representation of a late larval CNS as viewed from a ventral perspective. The larval CNS is composed of two brain hemispheres and the ventral ganglia. The primordium of the adult central brain (CB) develops in the medial regions of each hemisphere, while the adult optic lobes (OL) develop from primordia located laterally. B. Schematic drawing of one hemisphere showing the scattered distribution of CB NBs in the medial part, which proliferate from the first instar stage until the beginning of pupal development, and the LPC (Lamina precursor cells) and OPC (outer proliferation center) neuroepithelia located laterally. C. Representation of the OPC showing the symmetrically dividing neuroepithelial (NE) progenitors and the asymmetrically dividing NBs, which generate their progeny inside de OL. Double arrows indicate the direction of cell division. D. Representation of two CB NBs and their progeny. E. The typical pattern of division of type I CB and OPC NBs. Each NB divides asymmetrically several times to generate in each division a new NB and an intermediate progenitor called ganglion mother cell (GMC) which divides once to generate two postmitotic ganglion cells (GCs) that differentiate into neurons.

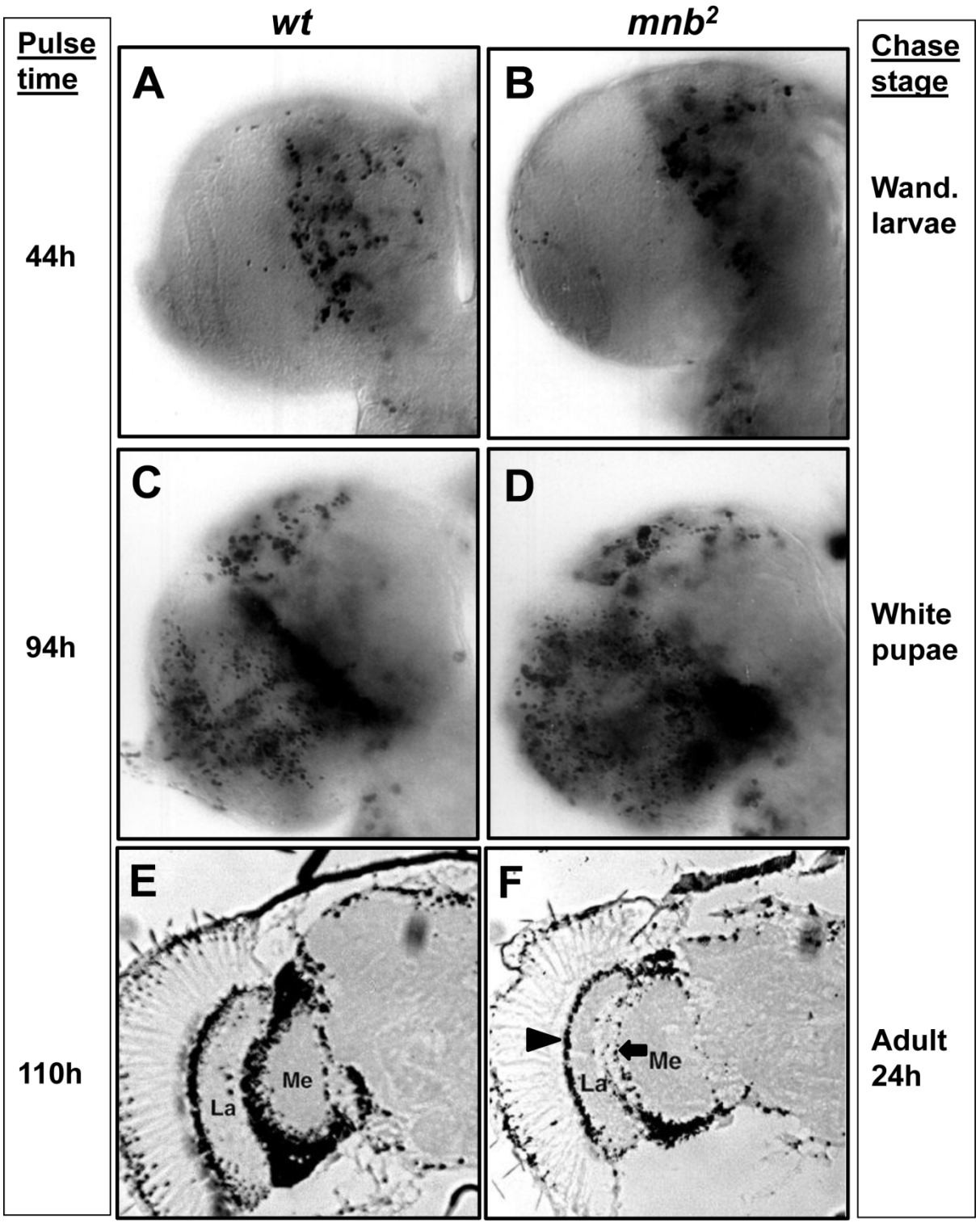

Suppl. Fig. S2. Pulse-chase BrdU labeling in *mnb* mutant.

in vivo BrdU labeling was carried out in order to determine at which step of larval development is generated the neuronal deficit of the *mnb* mutant. A single pulse of BrdU was applied *in vivo* to *wt* and mnb^2 larvae at the indicated times of larval development. This method allows the labeling of neurons at the time of birth. BrdU incorporation was analyzed in wandering larvae (A, B), white pupae (C, D) and in one-day-old adult brain frontal sections (E, F). Note that although the brain hemispheres of *mnb* larvae do not show any decrease in BrdU immunostaining in the optic lobe (OL) or central brain (CB) regions compared with the *wt* brain, the *mnb* adult brain (a section of one brain hemisphere) displays a strong decrease in the immunolabeling of the medulla cortex (Me, arrow) compared with the equivalent *wt* section (E, F). Also note that the lamina (La) cortex (arrowhead) is less affected. This is in agreement with the morphological phenotype in the brain of adult *mnb* mutants (Fischbach and Heisenberg, 1984; Tejedor et al., 1995). These results indicate that the neuronal deficit of *mnb* flies is mainly generated during the late larval or pupal stages.

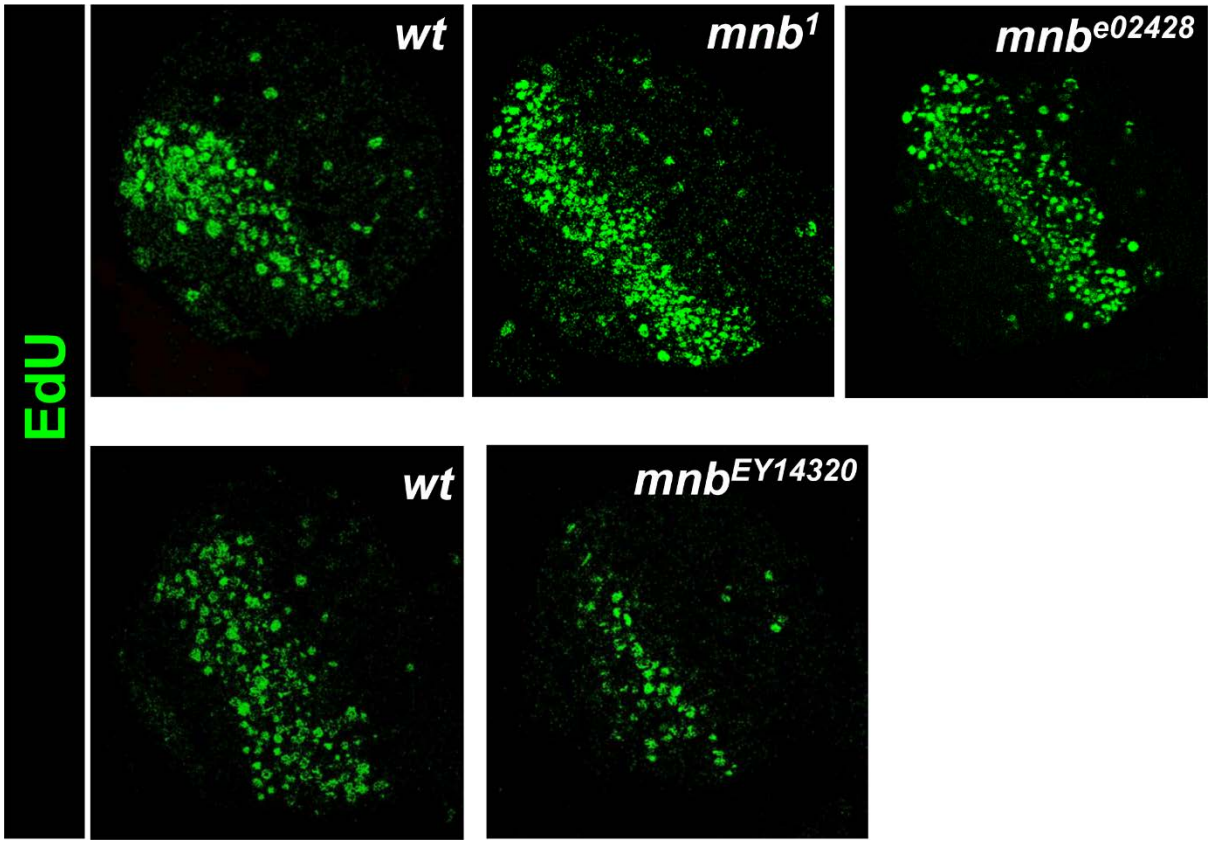

Suppl.Fig. S3. EdU labeling of *mnb* alleles.
Confocal images of wt, *mnb*^{1}, *mnb*^{e02428}, *mnb*^{EY14320} larval brains after a 7 min EdU pulse. Note the increase in EdU^{+} cells in *mnb*^{1}, *mnb*^{e02428} and the decrease in *mnb*^{EY14320}. Quantitative determination of EdU labeling is presented in Fig.1

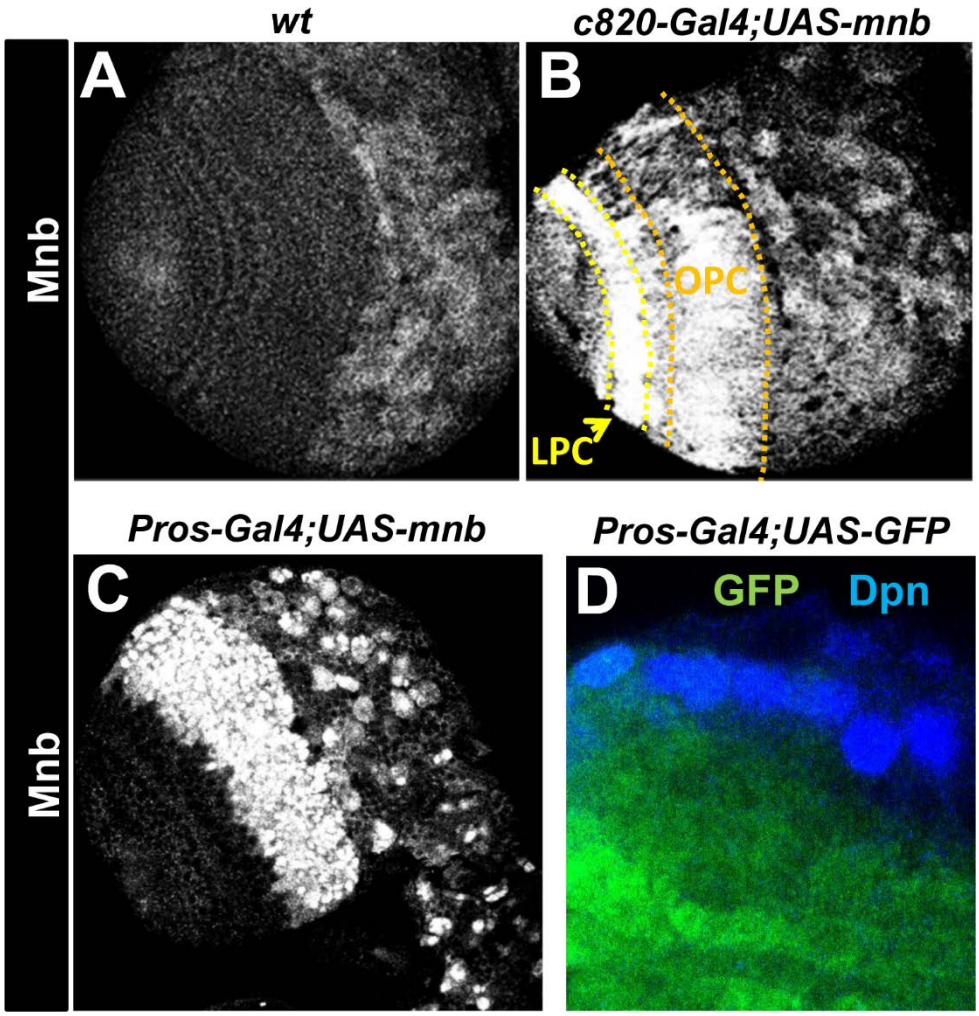

Suppl. Fig. S4. Expression patterns of Gal4 drivers
A,B,C, Confocal images taken from a ventro-anterior orientation through a brain lobe of *wt*, *c820-Gal4; UAS-mnb*, and *pros-Gal4; UAS-mnb* late third instar larvae showing Mnb immunolabeling. Note that the c820-Gal4 driver induces strong expression of Mnb in the LPC and OPC, and moderate in some CB areas. The *pros-Gal4* driver promotes strong expression of Mnb in the OPC while in the CB is variable depending on lineage. D. High magnification view of the OPC of a *Pros-Gal4;UAS-GFP* larval brain immunostained for DPN and GFP. Note that most GFP signal is inside the OL in Dpn^{-} cells.

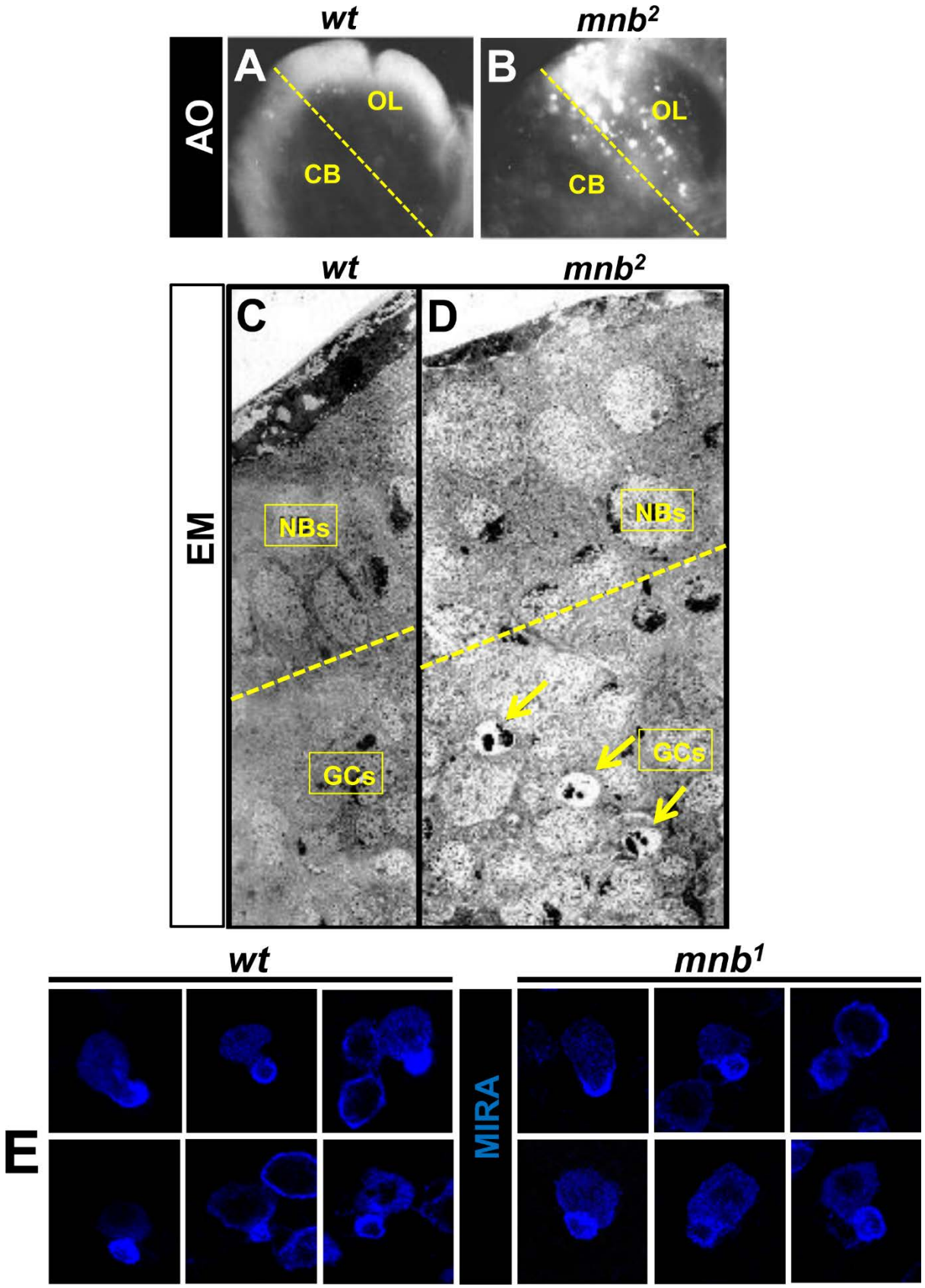

<u>Suppl. Fig. S5.</u> Additional cellular phenotype data of *mnb* mutants

Cell death was analyzed in the OL of *mnb*^{2} late-third-instar larvae using acridine orange (AO) staining (A, B) and electron microscopy (EM) (C,D). In the case of AO, images were obtained as projections of confocal sections through the brain lobes. Note the abundance of AO labeled cells in the *mnb* lobe compared with the wt lobe. EM images (C,D) were collected from frontal sections of larval OLs taken at the level of the OPC. Numerous pyknotic cells with fragmented and/or condensed nuclei (arrows) are located beneath the NBs in the *mnb* mutant OPC. E. High magnification views of representative CB NB lineages labelled with Mira. Note that in both *wt* and *mnb*^{1} only one small-medium strong Mira+ cell can be detected near the NB. This indicates that no apparent increase in GMCs number happens in *mnb* mutants.

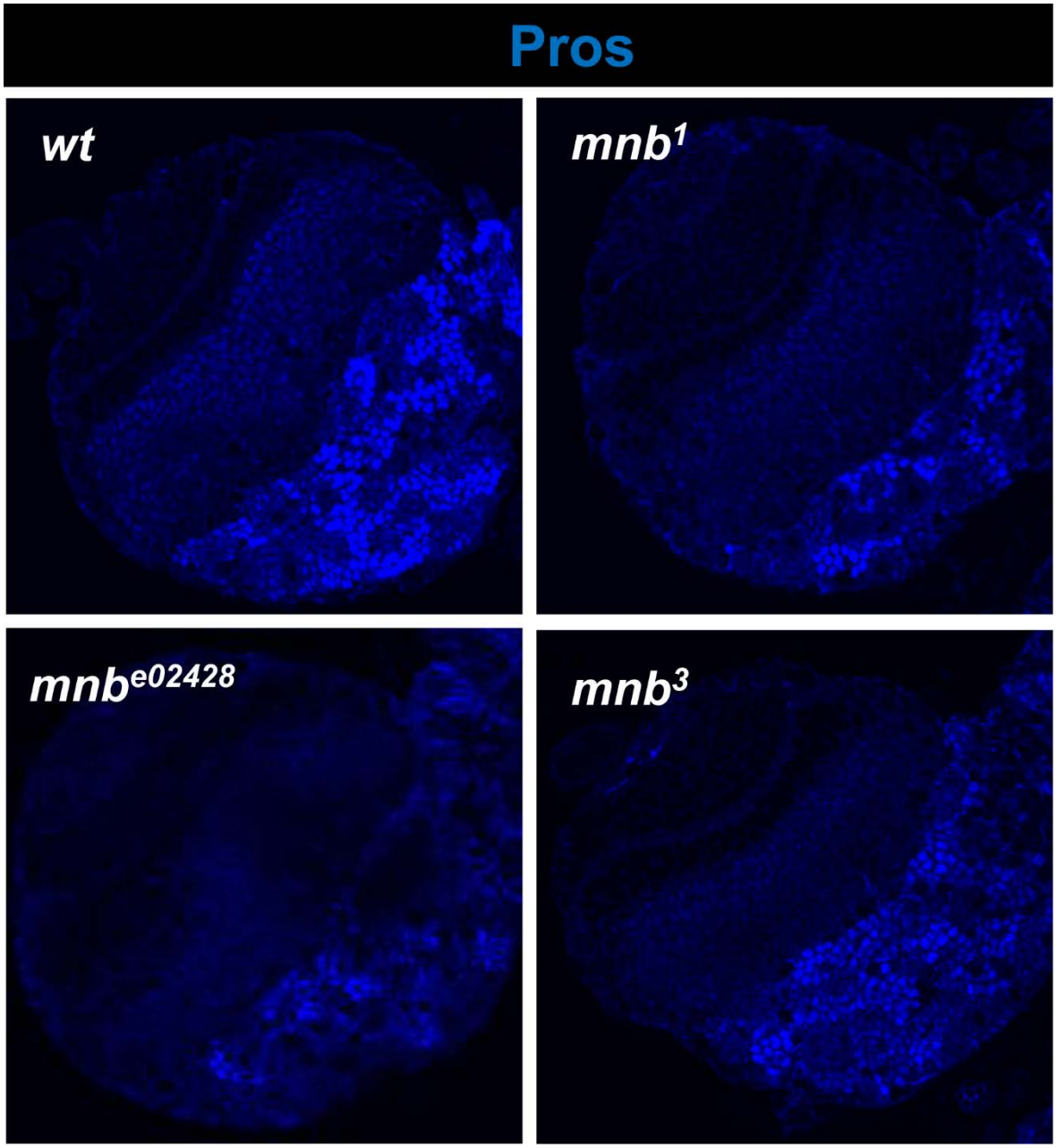

Suppl. Fig. S6. The expression of Prospero is decreased in LoF *mnb* alleles.
Confocal images of wt, *mnb*^{1}, *mnb*^{e02428}, *mnb*^{3} larval brains immunostained for Pros. Note the decreased labeling intensity in the three *mnb* alleles. Quantification of labeling intensity is presented in Fig.5.

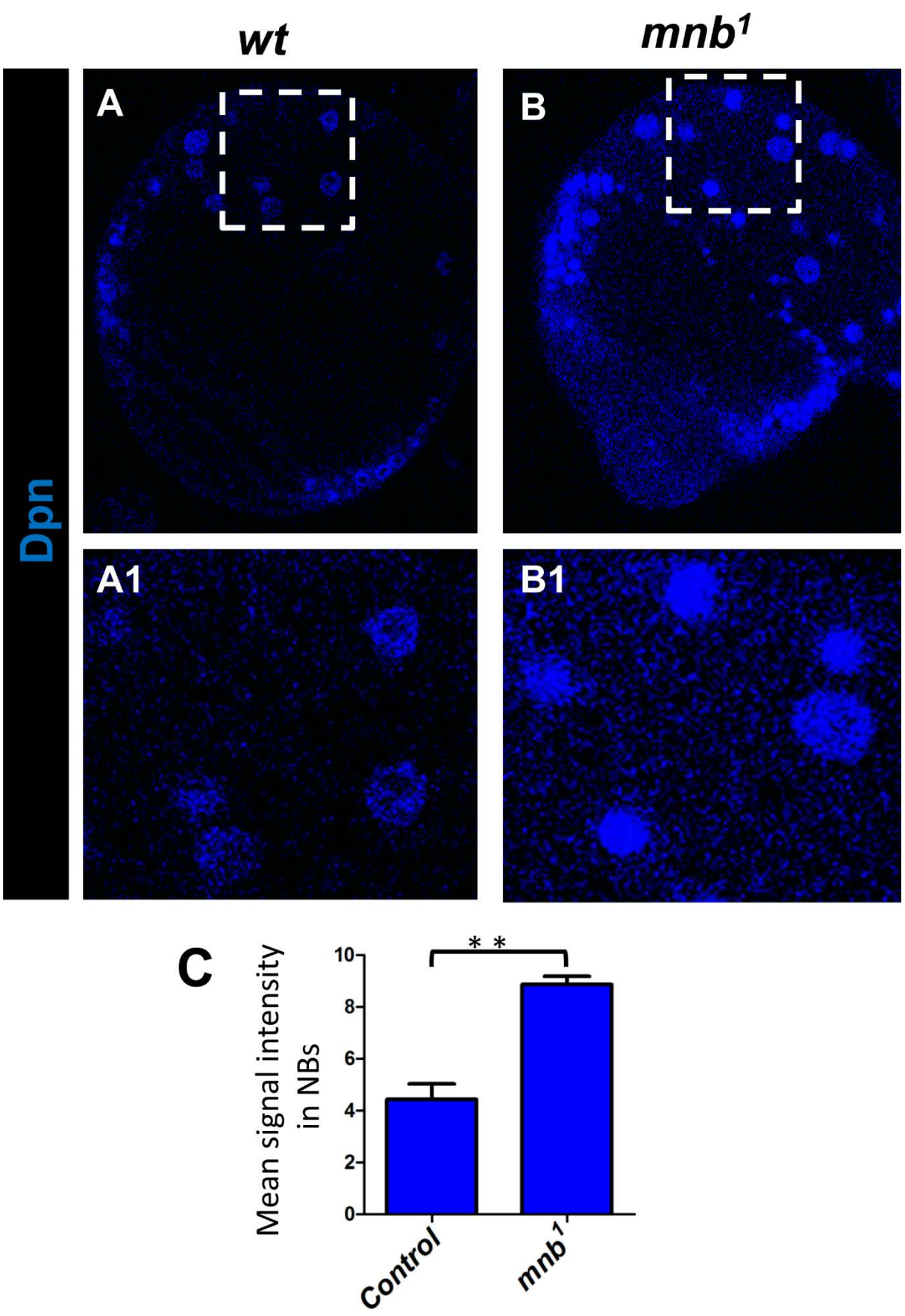

Suppl. Fig. S7. The expression of Deadpan is increased in NBs of *mnb* mutant.

A, B. Confocal images of wt and *mnb*^{1}, larval brains immunostained for Dpn. A1, B1. High magnification view of the framed regions in A and B. . Note the increase in labeling intensity in NBs of the *mnb* sample. Quantitative determination of labeling intensity was performed in 15 CB NBs in equivalent regions of 4 brain lobes of each genotype. Signal intensity was measured in 10µm diameter circles including each NB. (**, Statistic significance, $p < 0.0001$).

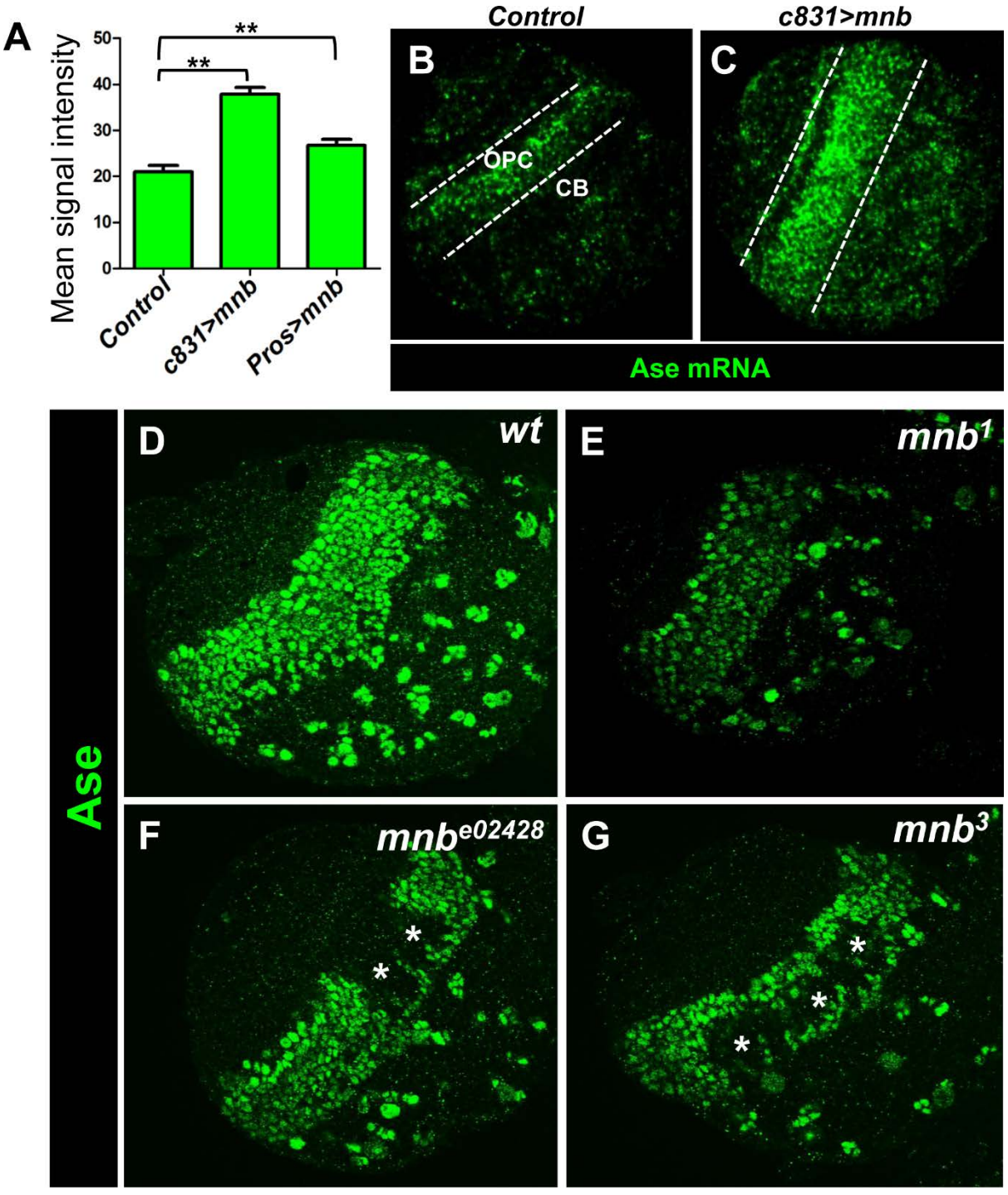

Suppl. Fig. S8. Changes in the expression of Asense in *mnb* LoF and GoF mutants.

A. Quantitative determination of Ase labeling intensity was performed in 4 brain lobes of each genotype. Representative images are shown in Fig.8 (**,Statistically significant, P< 0.0001). B, C. Partial confocal projection or serial images of larval brains after FISH of Ase. Note the strong increase in labeling after driving Mnb overexpression in the OPC with c831-Gal4. D-G. Confocal images of wt, mnb^{1}, mnb^{e02428}, mnb^{3} larval brains immunostained for Ase. Note the decreased labeling intensity in the three mnb alleles. In some cases, the decrease of Ase is particularly strong in some OPC cell clusters (asterisks).

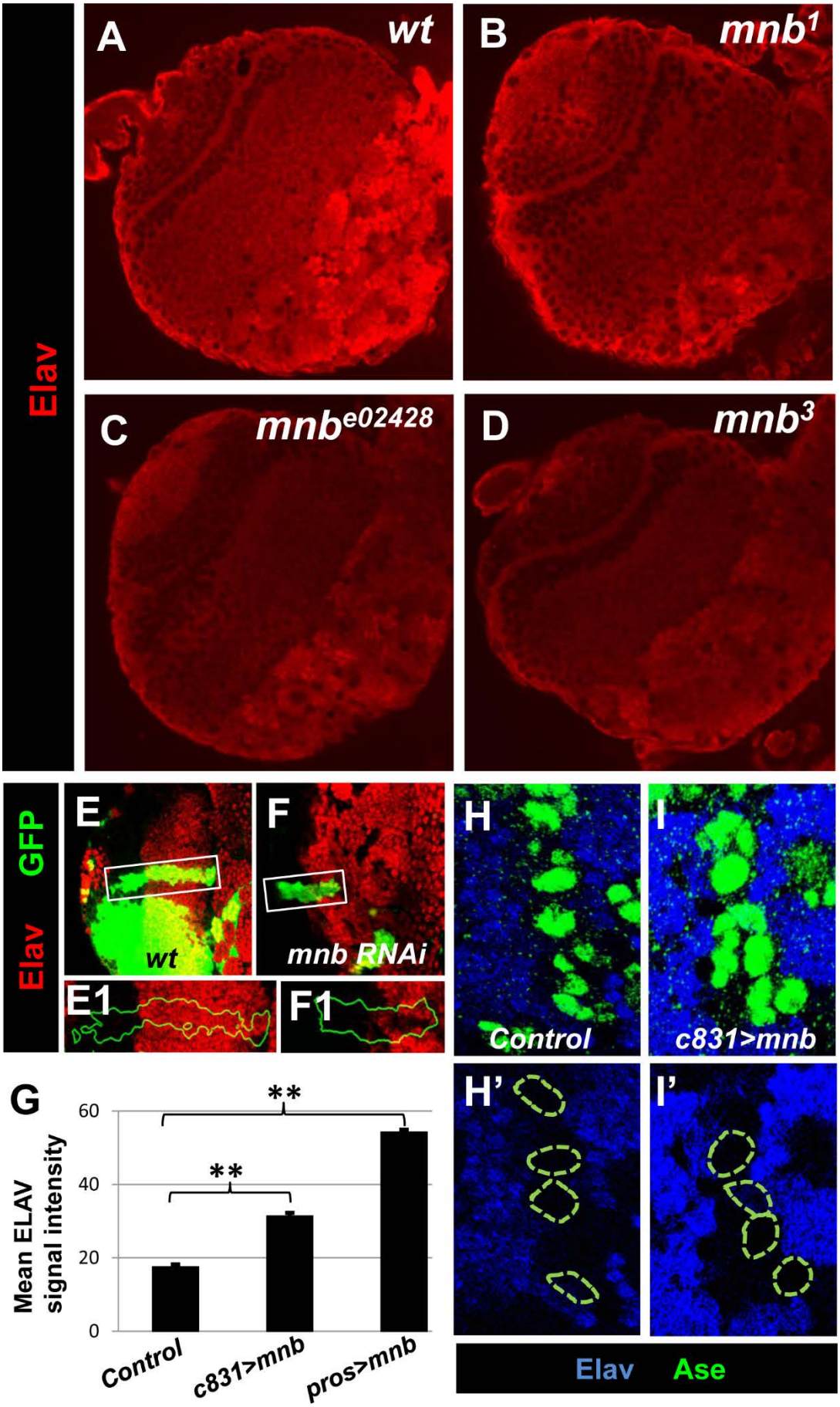

Suppl. Fig. S9. Effects of the LoF and GoF of *Mnb* on Elav expression.

A-D. Confocal images of wt, *mnb*^{1}, *mnb*^{e02428}, *mnb*^{3} larval brains immunostained for Elav. Note the decreased labeling intensity in the three mnb alleles. E,F. Mid magnification views of the OPC of larval brains in which *wt* and *UAS-mnb RNAi* clones expressing GFP were induced. Note the decrease in Elav staining inside the *mnb* RNAi clone. G. Quantitative determination of the Elav immunostaining intensity in larval brain lobes of *UAS-mnb* (control), *c831-Gal4;UAS-mnb*, and *pros-Gal4;UAS-mnb* late-third-instar larvae. (** Statistically significant, P <0.001). H,I. High magnification views of equivalent CB areas of *control* and *c831-Gal4; UAS-mnb* late third instar larval brains after activation at 29ºC for 10h. Note the increase in Ase signal in the NBs and of Elav in the surrounding GCs. However, Elav is not elevated in NBs (dotted circles).

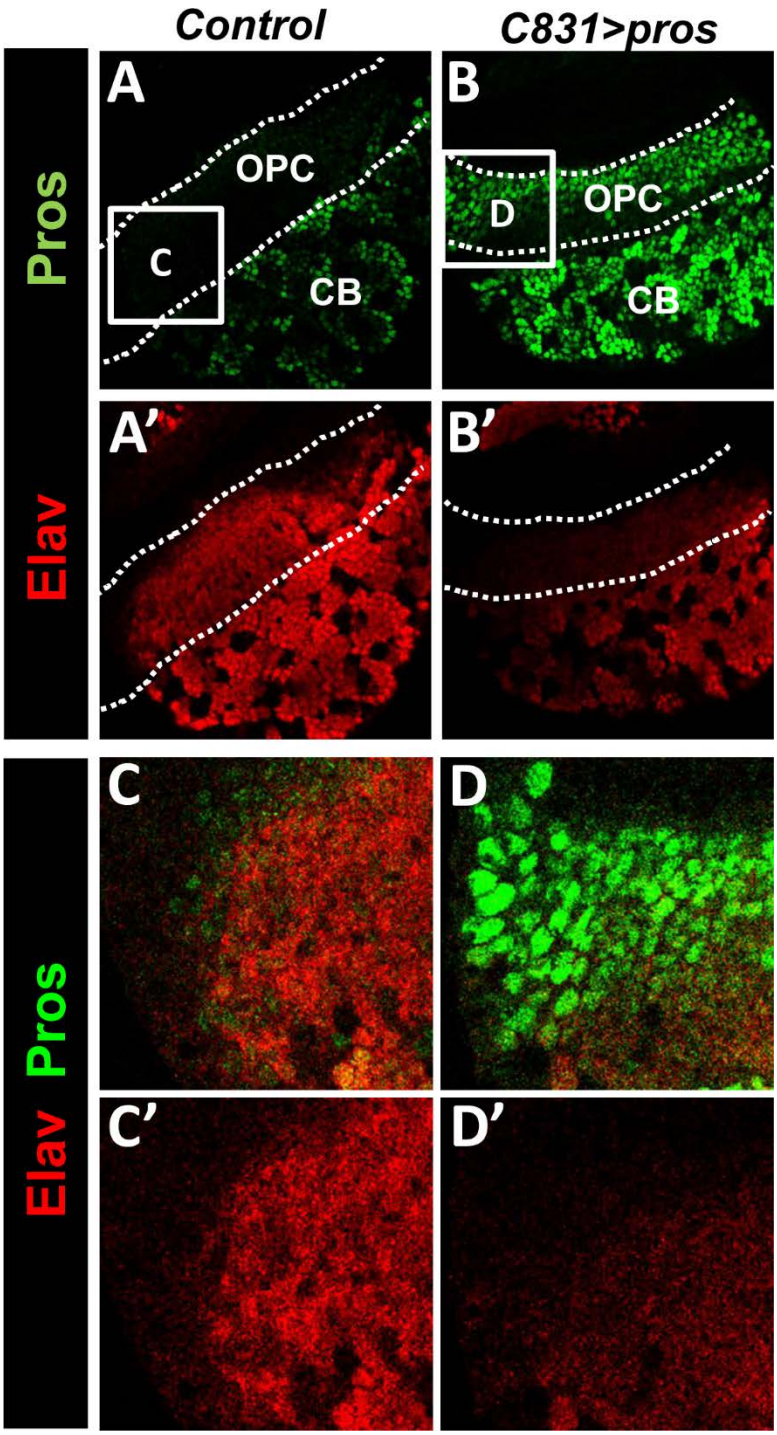

Suppl. Fig. S10. Effect of the GoF of *pros* on the expression of Elav.
A,B. Partial confocal projection images taken from a ventro-anterior orientation through the lobe of *wt* and *c831-Gal4; UAS-pros* late third instar larvae showing Pros and Elav immunolabeling. Note the increase in Pros level in the mutant OPC accompanied by some decrease in Elav. C,D. High magnification view of a single confocal section of the corresponding OPC areas framed in A and B, respectively. Notice the decrease in Elav in those cells with strong Pros labeling. This indicates that Pros might exert a suppression on *elav* expression. Nevertheless, we can not rule out that the decrease in Elav level could be an indirect effect due to the proliferation arrest of NBs and concomitant inhibition of neurogenesis that the GoF of *pros* causes (Colonques et al., 2011).

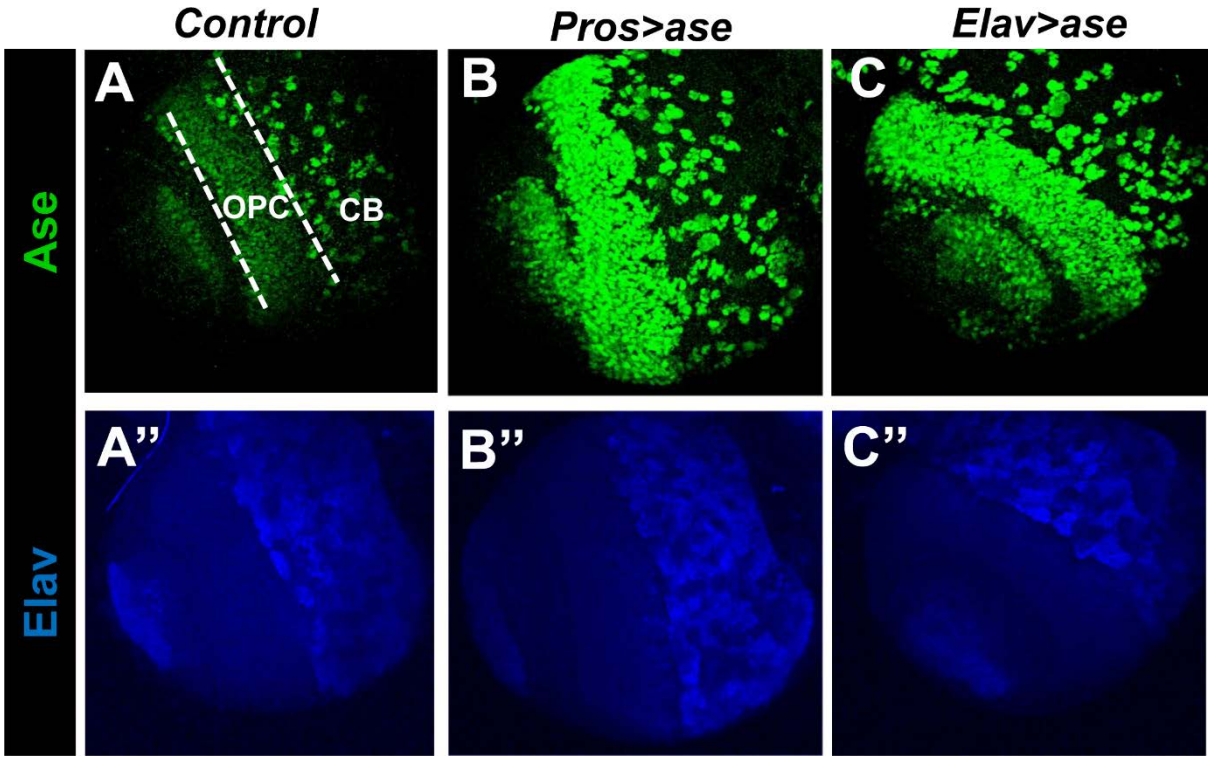

Suppl. Fig. S11. Effects of the GoF of *Ase* on Elav expression
A-C. Partial confocal projection images taken from a ventro-anterior orientation through the lobe of *Control*, *pros-Gal4;UAS-ase* and *elav-Gal4;UAS-ase* late third instar larvae showing Ase and Elav immunolabeling. Note that the strong induction of Ase both in the CB and OPC of the mutant lobes does not cause substantial changes in Elav labeling.

Supplementary Table S1. Information of *mnb* alleles

Allele	Genetic and Molecular nature	Phenotypes	Literature
mnb^{1}	Null Point mutation in kinase active site	Adult brain morphology BrdU labeling Cell death Expression of Cyclins Expression of Ase, Pros, Dap, Dpn, and Elav	Fischbach and Heisenberg, 1984 Tejedor et al, 1995 This paper
mnb^{2}	Strong hypomorph P-element insertion	Adult brain morphology BrdU labeling Cell death Expression of Cyclins Expression of Ase, Pros, Dap, Dpn, and Elav	Fischbach and Heisenberg, 1984 Tejedor et al, 1995 This paper
mnb^{3}	Strong hypomorph	Adult brain morphology BrdU labeling Expression of Ase, Pros, and Elav	Tejedor et al, 1995 This paper
mnb^{e02428}	P-element insertion Strong hypomorph	 EdU labeling Cell death Expression of Ase, Pros, and Elav	Parks et al., 2004; Thibault et al., 2004 This paper
mnb^{EY14320}	P-element insertion Mnb overexpression	 EdU labeling Expression of Cyclins	Bellen et al., 2004 This paper

References:

Bellen et al., 2004, Genetics 167(2): 761—781

Parks et al., 2004, Nat. Genet. 36(3): 288—92

Thibault et al., 2004, Nat. Genet. 36(3): 283--287 [